MedChemComm

RESEARCH ARTICLE

View Article Online
View Journal | View Issue

Cite this: *Med. Chem. Commun.*, 2017, **8**, 897

Recent trends in smart and flexible three-dimensional cross-linked polymers: synthesis of chitosan–ZnO nanocomposite hydrogels for insulin drug delivery†

Rasha E. El-Mekawy‡* and Rabab S. Jassas

Received 16th October 2016,
Accepted 9th January 2017

DOI: 10.1039/c6md00580b

rsc.li/medchemcomm

One set of major challenges and significant progress is attributed to the discovery of novel pharmaceuticals from the exoskeleton of marine crustacean wastes to minimize the environmental pollutants. In this strategy, high molecular weight chitosan was subsequently used in the synthesis of smart three-dimensional cross-linked network polymers. Super absorbent chitosan–ZnO nanocomposite hydrogels were synthesized *via* a terminated diisocyanate compound, a chitosan sample (NH_2/NCO), and ZnO nanoparticles in different concentrations (1–7%). The discovered intelligent drugs were confirmed by spectral analyses such as FTIR, XRD, DLS, TGA and morphological analyses such as AFM, SEM, and TEM. The unique physical properties of chitosan–ZnO nanocomposite hydrogels towards environmental stimuli and the porosity of their structures have gained particular interest in fluorescence isothiocyanate-labeled insulin-loaded hydrogel nanocomposites for *in vivo* drug delivery into the rat nasal cavity. Confocal laser scanning microscopy (CLSM) was used to prove the absorption enhancement of fluorescein isothiocyanate (FITC)-labeled insulin-loaded hydrogels in the rat nasal cavity by this formulation. The formulation of hydrogels apparently decreased the blood glucose concentration (50–65% of initial blood glucose concentration) for at least 4–5.5 h after administration, and no apparent cytotoxicity was found after administration.

1. Introduction

The efficacy of many drugs is often limited by their potential to reach the site of therapeutic action. In most cases (conventional dosage forms), only a small amount of the administered dose reaches the target site, whereas the majority of the drug is distributed throughout the rest of the body in accordance with its physicochemical and biochemical properties. Therefore, developing a drug delivery system that optimizes the pharmaceutical action of a drug while reducing its toxic side effects *in vivo* is a challenging task. Polymer hydrogels are still a new, rapidly developing group of materials gaining wide application in many fields, especially pharmacy, medicine, and agriculture.[1] Interestingly, hydrogels are three-dimensional, cross-linked networks of water-soluble polymers.[2–6] Hydrogels can be virtually made from any water-soluble polymer, encompassing a wide range of chemical compositions and bulk physical properties. Furthermore, hydrogels can be formulated in a variety of physical forms including slabs, microparticles, nanoparticles, coatings, and films. As a result, hydrogels are commonly used in clinical practice and experimental medicine for a wide range of applications, including tissue engineering and regenerative medicine,[7] diagnostics,[8] cellular immobilization,[9] separation of biomolecules or cells,[10] and barrier materials to regulate biological adhesions.[11] Polysaccharides can be obtained from a wide spectrum of plants and animals sources. Cellulose, chitin, and chitosan are polysaccharides and the most plentiful renewable resource in the world.[12] Chitosan is one of the derivatives of chitin, but some of its properties differ from those of chitin. Chitosan is soluble in most solvents, especially in an aqueous acidic solution, which enables it to behave as a cationic polyelectrolyte in highly concentrated acidic solution, and in this case, it will form quaternary ammonium salts; thus, it dissolves in water and not swell itself or in hydrogel structure. In recent years, chitosan has turned out to be preferable to chitin as it is more tractable in the solution process. Chitosan contains many properties common to biopolymers such as biocompatibility, biodegradability, and non-toxicity. However, it is unique because of certain properties such as film forming ability, chelation and absorption properties, and antimicrobial activity.[13] In addition, its great formability

Department of Chemistry, Faculty of Applied Science, Umm Al-Qura University, Makkah Al Mukarrama, Saudi Arabia

† The authors declare no competing interests.

‡ Permanent address: Department of Petrochemicals, Egyptian Petroleum Research Institute, Nasr City, Cairo, Egypt. E-mail: rashachemistry1@yahoo.com

enables it to be converted into fibers, films, coating, beads, powders, and solution, which allow it to be diverse in its usefulness.[13,14] The long-term objectives incorporated in this study are synthesizing water-retaining chitosan–ZnO nanocomposite hydrogels from high molecular weight chitosan, which was prepared from the exoskeleton of fishery wastes to act as a drug carrier of insulin Mixtard 30 to improve its quality in decreasing the blood glucose concentration by a formulation of hydrogels without the pain of injection.

2. Results and discussion

2.1. Chemistry

Nanotechnology is an emerging interdisciplinary technology that has been booming in many areas, including materials science, mechanics, electronics, optics, medicine, plastics, and aerospace, during the last decade.[15,16] Hydrogels are defined as hydrophilic polymers that, due to their structural network, can absorb water without being soluble under physiological conditions of temperature, pH, and ionic strength. Cross-links can be formed by covalent, electrostatic, or hydrophobic bonds, or dipole–dipole interactions.[17] In particular, hydrogels is a class of polymers that can absorb water or biological fluids and swell several times more than their dry volume. Dependence of the swelling behavior of the hydrogel on the changes in the external environment was reported.[18] Moreover, it was reported that the hydrogels can afford a free-space between the networks in the swollen stage that serves for nucleation and growth of nanoparticles and acts as nanoreactors or nanopots.[19] There is a significant interest in the development of hydrogel nanocomposites for a variety of biomedical applications including drug delivery, sensors and actuators, and hyperthermia cancer treatment. The incorporation of nanoparticles into a hydrogel matrix can result in unique material characteristics such as enhanced mechanical properties, swelling response, and capability of remote-controlled (RC) actuation. In this study, the development of hydrogel nanocomposites containing zinc oxide nanoparticles (ZnO), actuation with remote stimulus, and some of their applications have been highlighted. The chitosan–ZnO nanocomposite hydrogel thin films were designed by the solution casting method. The different concentrations of ZnO nanoparticles (1–7%), which have particle size of 159.7 nm, were added into chitosan (1 gm) and cross-linker (0.062 ml) solutions (Scheme 1). Subsequently, the solutions were homogenized at 1200 rpm to allow the homogeneous dispersal of ZnO nanoparticles through the sample solution. Then, all the samples were stirred in the presence of ultrasound radiation. The FT-IR spectrum showed a characteristic band at $\dot{\upsilon}$ 1630 cm^{-1} due to the presence of trace amounts of 20% carbonyl group of the acetyl group in the chitosan chain backbone, and this band provided a reasonable confirmation of the cross-linking reaction. ZnO nanoparticles were investigated by scanning electron microscopy, revealing spherical aggregates (SEM) (Fig. 1). Differential light scattering (DLS) measurements summarized that the size of the ZnO nanoparticles was 159.7 nm (Fig. 2) and atomic force microscopy (AFM) analyses can be used to form an image of the three-dimensional shape (topology) of a sample surface at a high resolution, with the determination of the nanometer size of zinc oxide particles (Fig. 3).

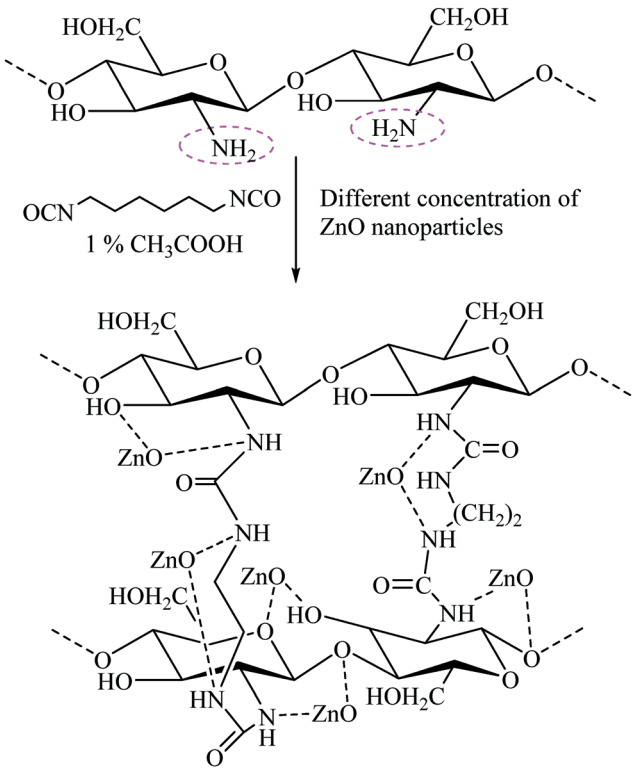

Scheme 1 Schematic of the cross-linking between chitosan, ZnO nanoparticles, and cross-linker (hexamethylene-1,6-diisocyanate).

In particular, chitosan–ZnO nanocomposite hydrogel thin films were confirmed by transmission electron microscopy (TEM) (Fig. 4). TEM illustrates that 2, 4, and 5% ZnO nanoparticles were loaded into chitosan hydrogel films. Periodically, scanning electron microscopy (SEM) (Fig. 5 and 6) of hydrogel films before and after swelling exhibited the porosity and possibility of loading aqueous medium into porous parts, leading to excellent swelling. In detail, the SEM image of 2% (a), 3% (b), 4% (c), and 5% (d) of ZnO nanoparticles before swelling illustrates the porosity of films, and this permits the loading of drugs into the gel films (Fig. 5).

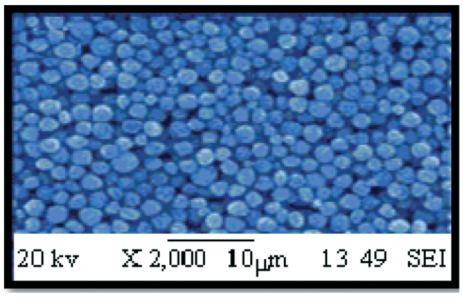

Fig. 1 SEM image of ZnO nanoparticles comprising spherical aggregates with a monodispersed size distribution.

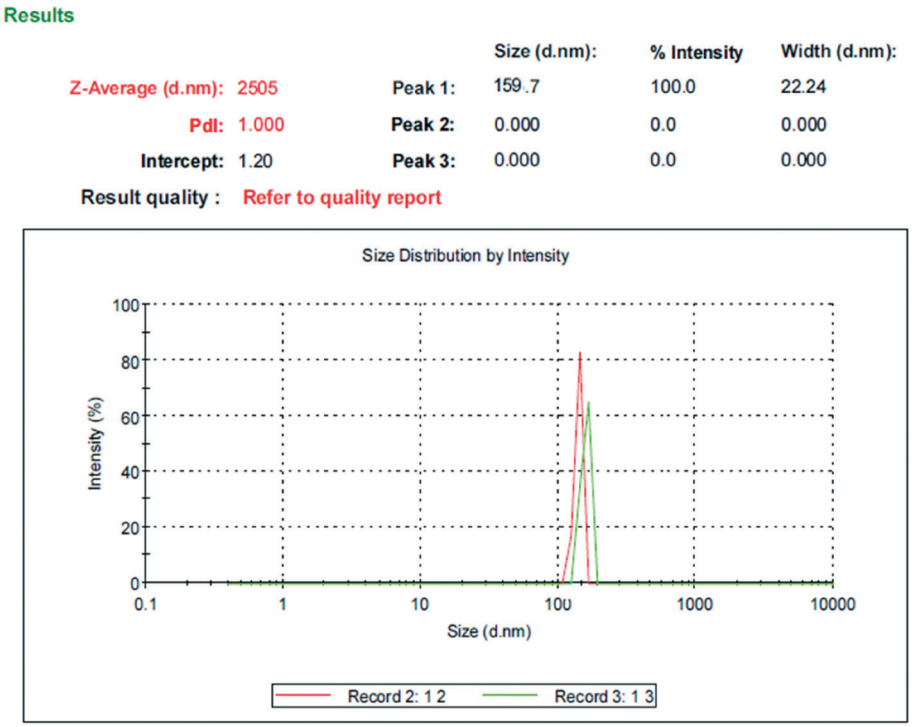

Fig. 2 Differential light scattering (DLS) of ZnO nanoparticles at 159.7 nm.

X-ray diffraction measurements exhibited a purity of samples and thus it showed a high crystallinity of chitosan–ZnO nanocomposite hydrogels and also demonstrated the type and shape of chitosan structure, which incorporated in the hydrogel structures in space; it showed the presence of alpha and gamma chitosan units, which act as building blocks of a backbone of super absorbent polymer nanocomposites at 2%, 4%, and 5% of ZnO nanoparticles (Fig. 7). Chitosan–ZnO hydrogels were assigned by thermal gravimetric analysis (TGA) which revealed the thermal stability of the synthesized network polymers. It showed different weight loss at different temperatures. The first decomposition peak of hydrogels containing 4% ZnO nanoparticles is observed in the range 43.68–229.43 °C due to moisture vaporization. The other weight loss at 238.97–434.66 °C is due to the first degradation of the chitosan molecule (glycosidic linkage). The final weight loss at 485.18–767.18 °C is due to the decomposition of glucosamine rings (Fig. 8).

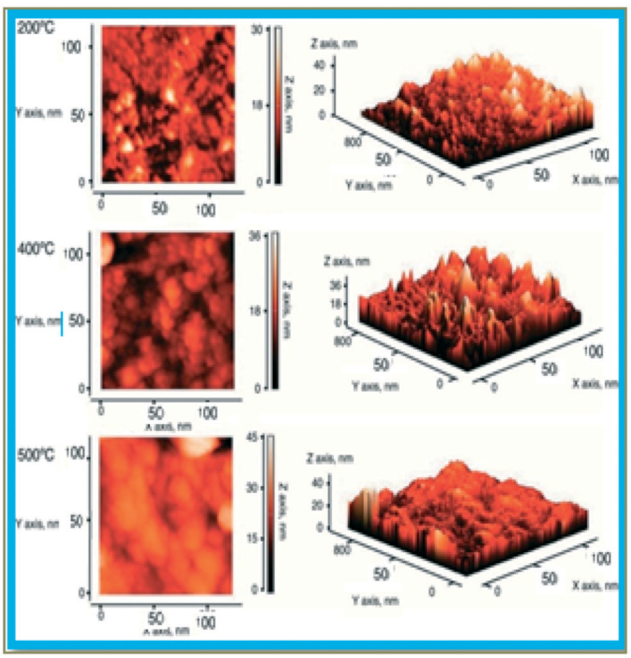

Fig. 3 Atomic force microscopy (AFM) of ZnO nanoparticles.

2.2. Kinetic study of the cross-linked polymer (chitosan hydrogel)

2.2.1. Responsive-stimuli of chitosan–ZnO nanocomposite hydrogel.

2.2.2. Swelling studies of water retaining nanocomposite hydrogels at different temperatures, in acidic and basic media at different pH values. Stimuli-sensitive hydrogels are interesting to use as new intelligent materials due to their capacity for swelling and deswelling according to the conditions. There are three functions of gels in biomedical field applications: (a) sensing an external signal (sensor function), (b) evaluation (processor function), and (c) action (actuator function), which were developed as intelligent gels or smart gels. The functions of stimuli-responsive gels can be roughly classified into three categories: (a) mechanical motion, (b) mass transport, and (c) conversion and transmission of

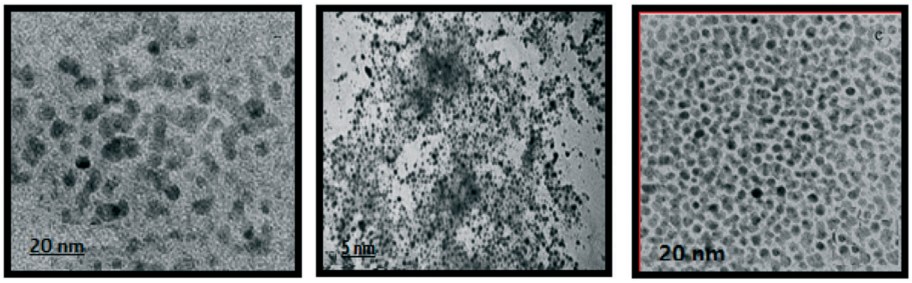

Fig. 4 TEM images of chitosan–ZnO nanocomposite hydrogels at (2, 4, and 5% ZnO nanoparticles), respectively.

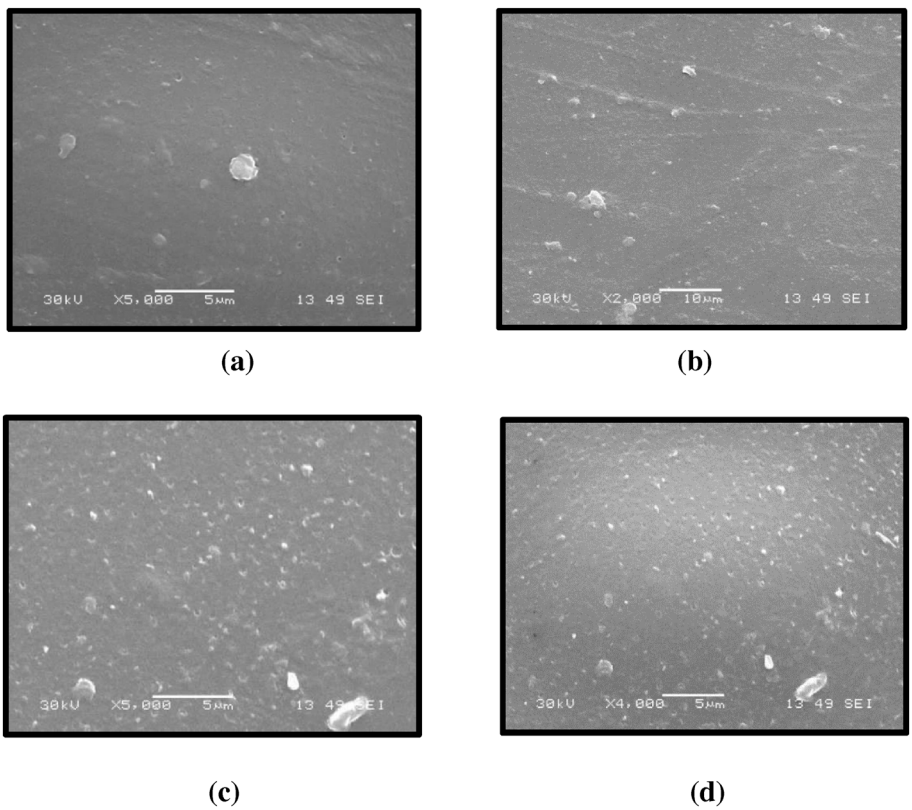

Fig. 5 SEM images of nanocomposites before the swelling test (2% (a), 3% (b), 4% (c), and 5% (d) of ZnO nanoparticles).

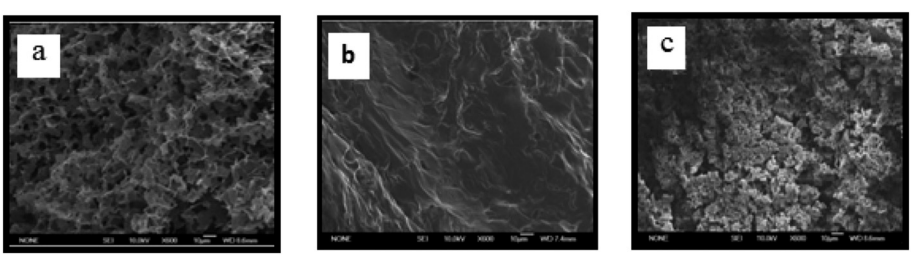

Fig. 6 SEM images of nanocomposites after the swelling test ((a) 2%, (b) 4%, and (c) 5% of ZnO nanoparticles).

information.[19] Controlled drug delivery can use these categories to achieve (1) constant concentration of therapeutically active compounds in the blood with minimum fluctuations; (2) predictable and reproducible release rates over a long period of time; (3) protection of bioactive compounds considering their very short half-life; (4) elimination of side-effects, waste of drug, and frequent dosing; (5) optimized therapy and better patient compliance; and (6) solution of the drug stability problem.[20] The following section describes pH, temperature, and some of the biochemical analytes as

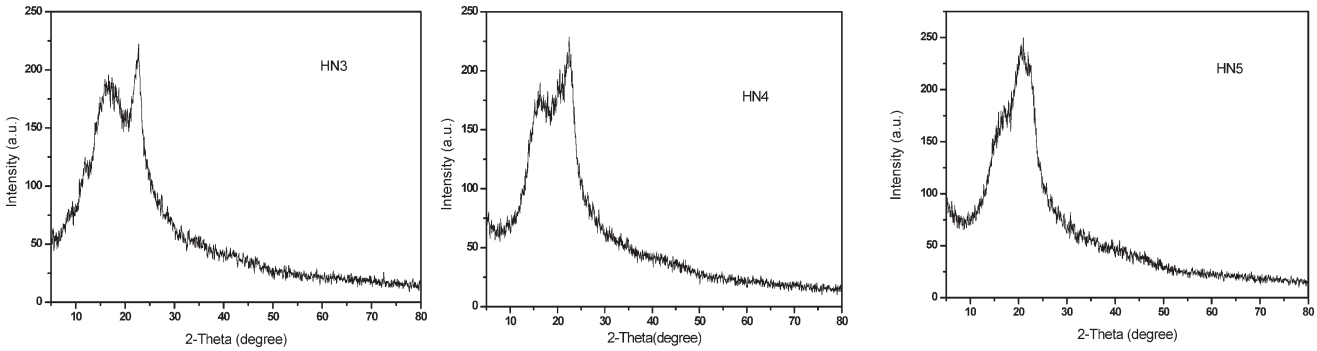

Fig. 7 X-ray diffraction (XRD) of chitosan–ZnO nanocomposite hydrogel (2%, 4%, and 5% of ZnO nanoparticles), respectively.

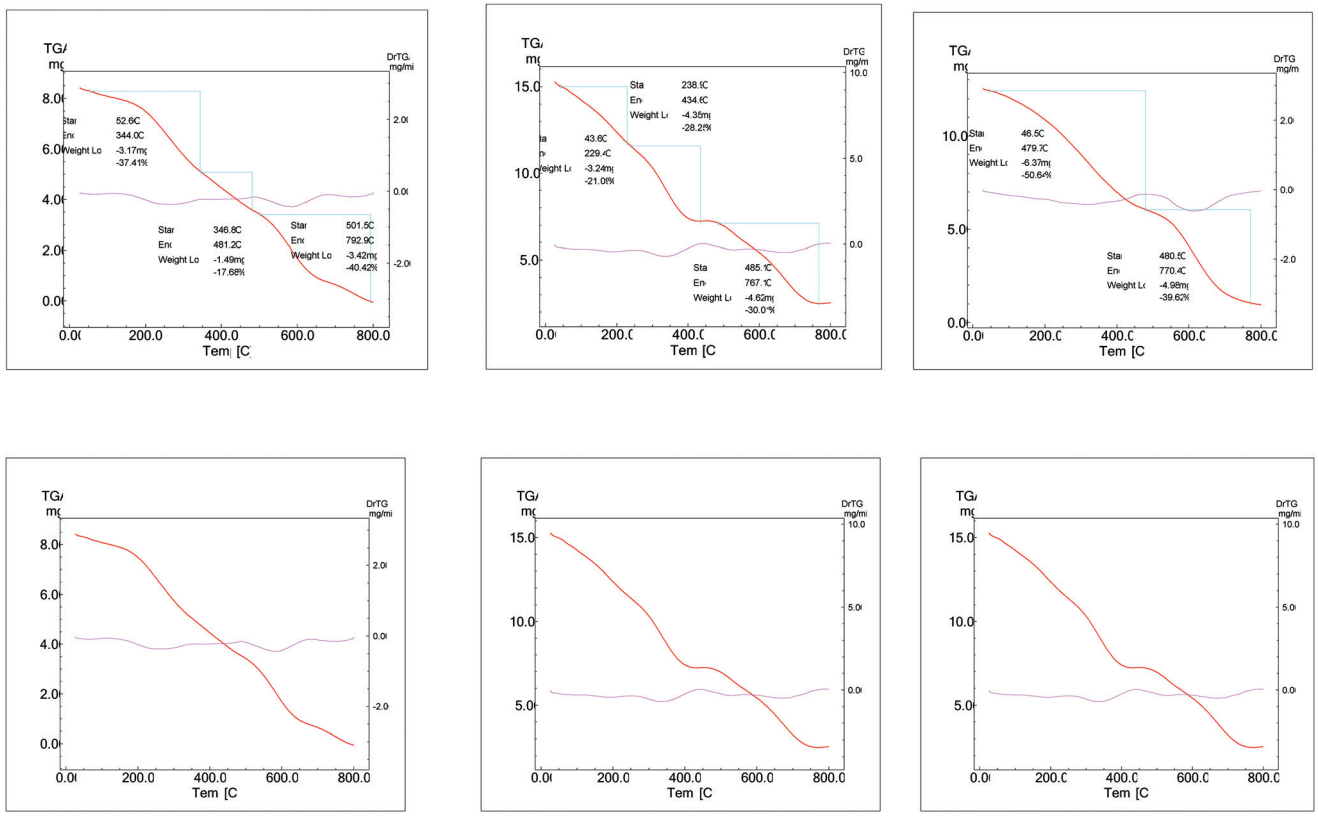

Fig. 8 TGA of chitosan–ZnO nanocomposite hydrogel (2%, 4%, and 5% of ZnO nanoparticles), respectively.

representative stimuli modulating the volume transitions in smart polymeric gels. We investigated the water uptake of dried nanocomposite hydrogel samples in different aqueous solutions as a preliminary application for the main application of drug delivery. Moreover, these applications provided an impression about the suitable conditions required for insulin drug-delivery application. The swelling equilibrium age percentage was calculated as follows (Fig. 9–11):

$$\text{Swelling Equilibrium Percentage } (S\%) = \frac{W_s - W_d}{W_d} \times 100$$

where W_s is the weight of swollen hydrogels and W_d is the weight of dried hydrogels.

2.3. Pharmaceutical applications of hydrogels

2.3.1. Extending the effectiveness of hydrogels for insulin drug-delivery into rat nasal cavity.

2.3.2. Incorporation of insulin (Mixtard 30) into hydrogels during their design. The interest in RC drug delivery from hydrogel nanocomposites using a variety of approaches is increasing. Millions of people who suffer from insulin-dependent diabetes mellitus (IDDM) or non-insulin-dependent diabetes mellitus (NIDDM) have to be injected with insulin to maintain their blood glucose concentration

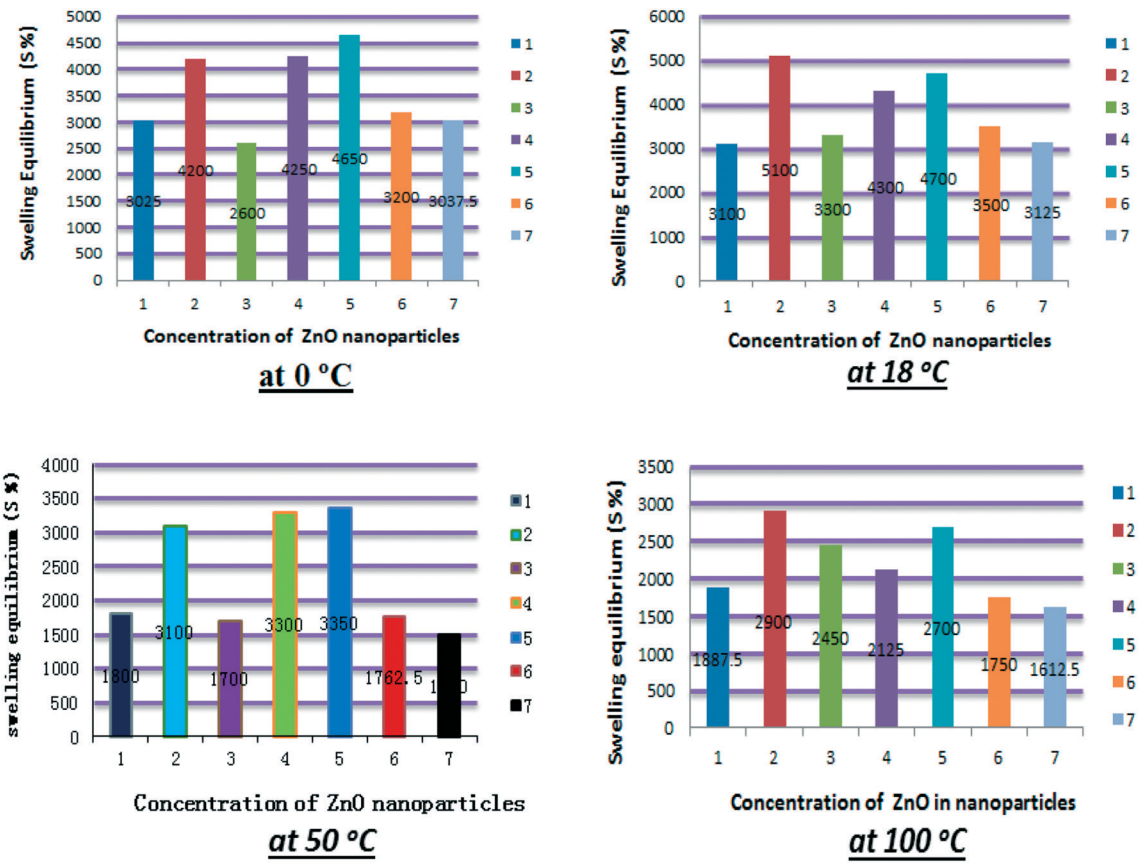

Fig. 9 Swelling equilibrium of nanocomposite hydrogels at pH = 7 (water medium) at different temperatures 0, 18, 50, and 100 °C.

within the normal range. The patients with IDDM, in particular, have to receive several injections every day, which causes pain and inconvenience. In addition, fluctuation of blood glucose concentration can result from the frequent intramuscular or subcutaneous injections of insulin, which can sometimes lead to the exacerbation of some diabetes complications.

The extensive study of nasal insulin administration as an alternative route improved the blood glucose concentration control. The available nasal devices originally designed for solution formulation were used to drop or spray the formulation easily into the rat nasal cavity and the formulation could widely spread on the nasal mucosa in the solution state. The solution transformed to viscous hydrogel, because of the elevated temperature (37 °C) in the nasal cavity, which can reduce the mucociliary clearance rate from the nasal cavity and slowly release the drug, as soon as it comes into contact with the nasal mucosa. This formulation enhanced the absorption of fluorescein isothiocyanate (FITC)-labeled insulin in the rat nasal cavity and the confocal laser scanning microscopy (CLSM) was used to confirm this.

The nanocomposite hydrogel formulation apparently decreased the blood glucose concentration (50–65% of the initial blood glucose concentration) for at least 4–5.5 h after administration. No apparent cytotoxicity was found after administration because the tested hydrogels were ecofriendly and healthy. The drug did not appear to cause adverse effects on the rat nasal cavity cell membrane and cell nuclei, owing to the homologous shape of cell membrane and cell nuclei. The overall observations were really related to the high molecular weight of polymer chains and also to the porosity of their film surfaces, which permitted the loading of insulin into the gel matrix (Fig. 12 and 13).

3. Experimental

3.1. General remarks

Preparative chitosan from shrimp shell obtained with a degree of deacetylation (DD) of 80% and an average molecular weight of 800 000 kDa was used. X-ray diffraction (XRD) was employed for the investigation of the crystallinity of the polymer. X-ray diffraction was performed using a Philips model PW 3710 (Philips, USA) diffractometer with CuKα radiation (λ = 0.1542 nm) in a sealed tube operated at 40 kV and 30 mA. The diffraction patterns were obtained from 10 to 80 2-theta degree at a scanning rate of 1 min^{-1}. The basal spacing of the silicate layer, d, was calculated using the Bragg's equation, $k = 2d \sin\theta$ (where θ is the diffraction position and k is the wavelength). The scan speed (2θ s^{-1}) of 0.040 s^{-1} was used. Scanning electron microscopy (SEM) was performed using a Philips model XL 30CP, USA. The films were cut and mounted on brass stubs with double-sided adhesive tape and

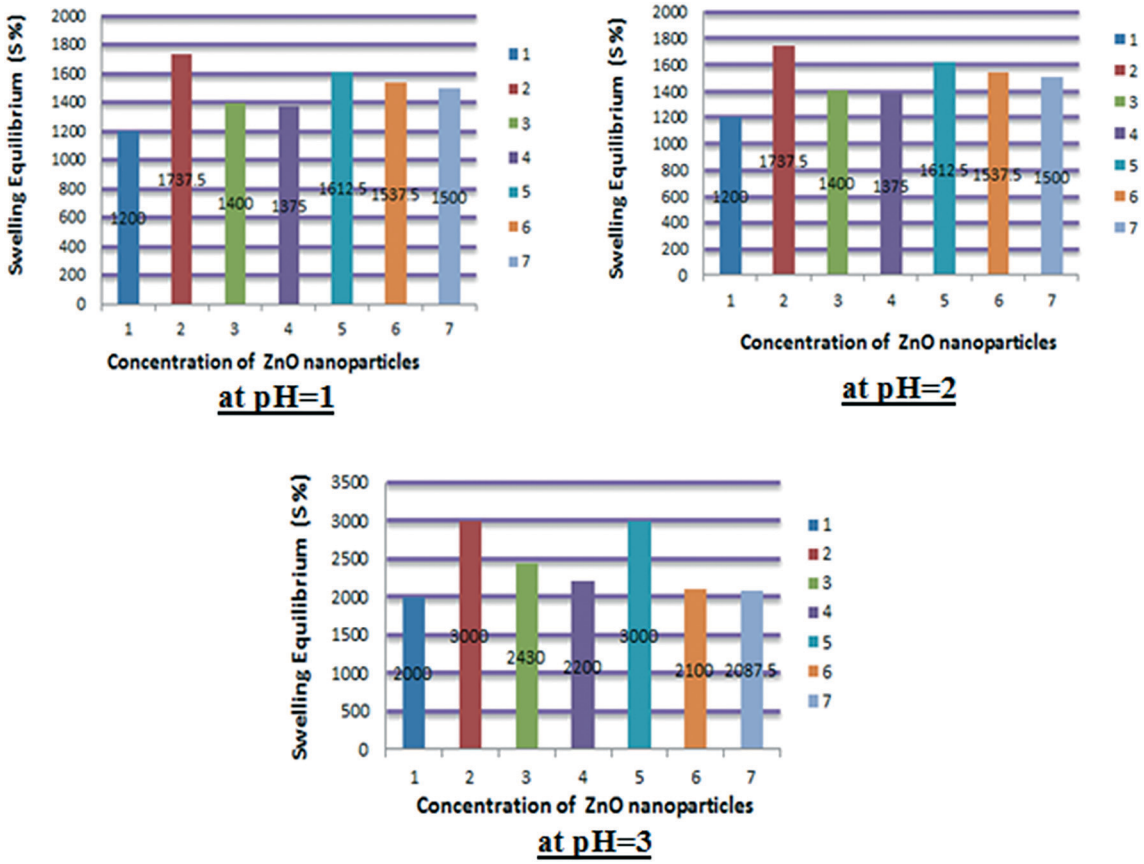

Fig. 10 Swelling equilibrium of nanocomposite hydrogels at pH = 1, 2, and 3 (acidic medium).

were coated with 50 Å of gold vapor using an SCD-040 Balzers sputter. The specimen was finally characterized by SEM using an accelerating voltage of 20 and 30 kV and a 2000×, 4000×, and 5000× magnification of the original specimen size. All the experiments were performed in compliance with the relevant laws and guidelines of Umm Al-Qura University, Faculty of Science, Chemistry Department in the Kingdom of Saudi Arabia and the institutional committee(s) in Umm Al-Qura University has approved the experiments. In addition, the spectral analyses were performed in the King Khaled University, Faculty of Science, Saudi Arabia. Moreover, the biological activity of the tested hydrogels was tested in the Pharmacognosy Department, Faculty of Pharmacy, Mansoura University. The used rats were purchased from the National Center of Research and all the chemicals were purchased from Sigma Aldrich.

3.2. Synthesis

3.2.1. Synthesis of chitosan–ZnO nanocomposite hydrogels. In a round-bottom flask equipped with a chemical stirrer, chitosan of high molecular weight (800 000 kDa) was dissolved and stirred in 1% (w/v) of acetic acid for about 1 h, and then the terminated NCO of hexamethylene 1,6-diisocyanate (HMDI) NCO/NH_2 (0.062 ml) was slowly added under stirring for about 30 min. Moreover, different concentrations of ZnO nanoparticles (1%, 2%, 3%, 4%, 5%, 6%, and 7%) were added to the reaction mixture, and then the reaction was continued and carried out at 40 °C for 5 h. All the samples were then ultrasonicated by stirring under ultrasound radiation. The reaction mixture was filtered off to remove the unreacted material. The film solution was cast onto a 7 cm Petri dish and allowed to dry at room temperature (23 °C) for 7 days. Then, the thin films were separated as transparent films, as depicted in Fig. 14 and 15.

3.2.2. Swelling of the synthesized hydrogel–ZnO nanocomposites. In a 100 ml beaker, a specific weight of each sample (0.08 g) was taken and added to 50 ml distilled water at different temperatures (0, 18, 50, and 100 °C), different degrees of acidity (pH = 1, 2, and 3) and basicity (pH = 11.9, 12.4, and 13.9). Each sample was then left in different aqueous solutions to completely swell. After this, each swollen sample was weighed. The swelling equilibrium percentage (S%) for each sample was calculated, and the relationship between ZnO concentrations and swelling equilibrium percentage (S%) was graphed.

3.2.3. Scanning electron microscopy. Specimens of hydrogel nanocomposites were mounted on stubs appropriate for the particular scanning electron microscope being used. A convenient adhesive of double-stick, electrically-conductive carbon tape was used. To assure electrical continuity of the specimen with the stub, a small drop of silver paint may be

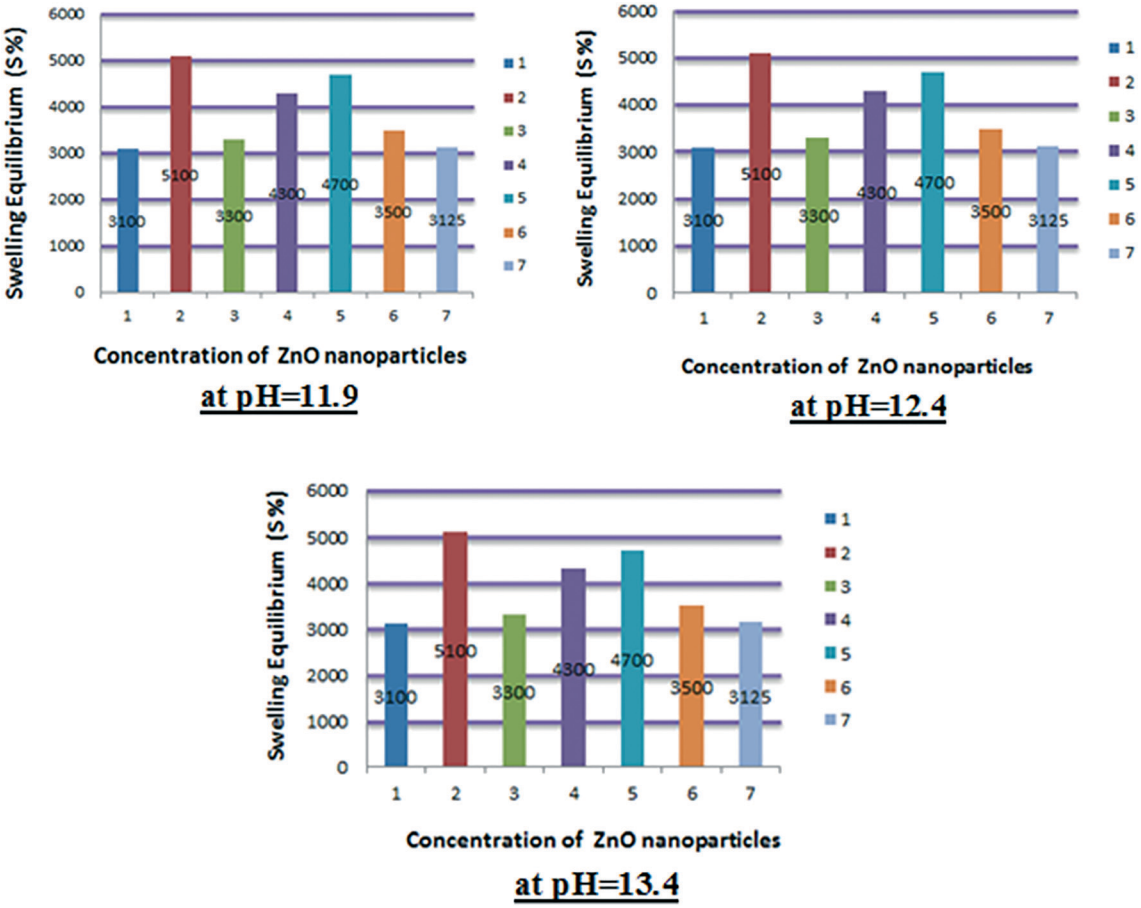

Fig. 11 Swelling equilibrium of nanocomposite hydrogels at pH = 11.9, 12.4, and 13.4 (basic medium).

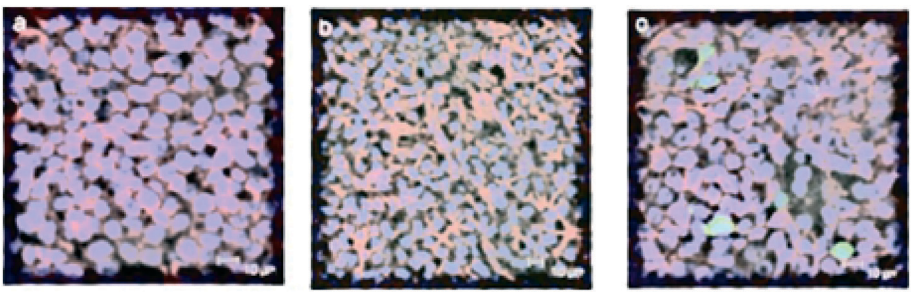

Fig. 12 CLSM images of rat nasal epithelia following the administration of FITC-insulin solution in PBS (a), FITC-insulin (b) FITC-insulin solution-loaded chitosan–ZnO nanocomposite hydrogel (0.062) (2%) solution, (c) and FITC-insulin solution-loaded chitosan–ZnO nanocomposite hydrogel (0.062) (5%) solution at λ (400–440, 510–550, and 560–600 nm).

added *via* the critical point drying technique. A critical point drier (CPD) was used to replace all ethanol with liquid carbon dioxide under pressure. The pressure and temperature were increased in the CPD until the specimen was above the triple point, at which time, it is safe to decrease the temperature and release the pressure. The volume of liquid carbon dioxide was replaced several times until ethanol was no longer present in the purge line. One or two additional replacements with liquid carbon dioxide were typically used to ensure that no ethanol was present during the drying stage. Once the dried material was removed, it needed to be stored in a desiccated environment until analyzed.

3.2.4. Thermal gravimetric analysis. The samples were subjected to a controlled heating/cooling program (non-isothermal or isothermal) and their weights were measured over time at different temperatures.

3.2.5. Incorporation of insulin and *in vitro* release study. The same procedure of chitosan hydrogel with cross-linker

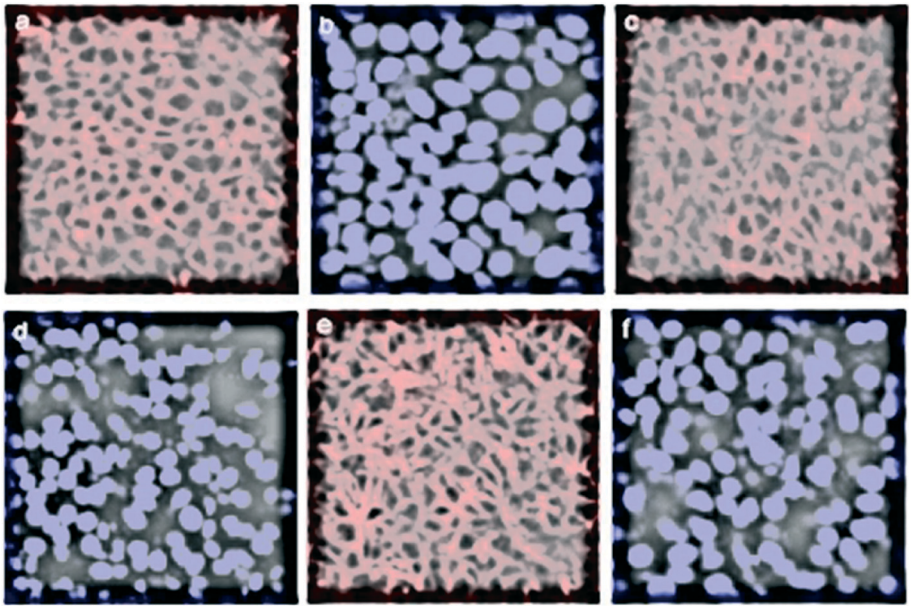

Fig. 13 CLSM images of the rat nasal epithelia treated with PBS (pH 7.4) [(a) cell membrane, FITC-insulin, (b) cell nuclei], FITC-insulin [(c) cell membrane, (d) cell nuclei], chitosan–ZnO nanocomposite hydrogel (0.062, 2%) solution [(e) cell membrane, (f) cell nuclei], chitosan–ZnO nanocomposite hydrogel (0.062, 5%).

(0.062 ml) and ZnO nanoparticles (2 and 5%) was used, apart from the addition of different concentrations of insulin Mixtard 30 (1%, 2%, 3%, 4%, 5%, 6%, and 7%). All the samples were then ultrasonicated by stirring under ultrasound radiation.

3.2.6. Fluorescein isothiocyanate labeling of insulin. Fluorescein isothiocyanate (FITC) was covalently bound to insulin as previously described.[16] Briefly, a solution of FITC in dimethylsulfoxide (5 mg mL^{-1}) was slowly added in a 5 mL insulin solution (8 mg mL^{-1}, 0.1 M Na_2CO_3). After an incubation period of 10 h at 10 °C, the coupling reaction was stopped by adding 10 mL NH_4Cl (50 mM). The mixture was stirred for 2 h at 4 °C. Ultrafiltration was performed to separate the unbound FITC. The FITC-insulin conjugate was frozen at −30 °C, lyophilized, and stored at 4 °C in the dark until further use.

3.2.7. Staining and visualization of samples by confocal laser scanning microscopy (CLSM). The samples of the nasal septum were stained with rhodamine-labeled phalloidin and Hoechst 33258. The samples were placed on a slide glass and the slide was then with a cover glass. After this, the samples were observed using a TCS SP2 CLSM (Leica, Germany) to visualize the permeation of FITC-insulin. FITC, Hoechst 33258, and Rhodamine were excited at 488, 365, and 543 nm, respectively. Three fluorescent images were obtained at different wavelengths (410–440, 520–550, and 560–600 nm).

3.2.8. Viability of the cells using propidium iodide (PI). Using a similar procedure to that adopted for the drug administration, a 25 mL sample was daily administered into the nasal cavity. After administration for 1 week, 50 mL PI in a buffer saline solution (PBS) of 30 mg mL^{-1} was applied by micro-injector for 20 min. To remove the non-penetrative PI, the nasal cavity was extensively washed by ice-cold PBS buffer at the rate of 2 mL min^{-1} by a peristaltic pump for at least 1 h. The rats were then euthanized, and the nasal septum was carefully isolated and washed with ice-cold PBS. After being put on a slide glass and being covered with a cover glass, the samples were excited at the wavelength (λ) of 550 nm by CLSM, and fluorescent images at 560–600 nm were obtained.

4. Conclusion

From the abovementioned discussion, it may be concluded that it is worthwhile to synthesize intelligent chitosan–ZnO

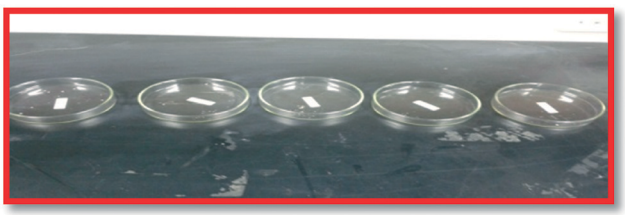

Fig. 14 Thin films before separation from Petri dish.

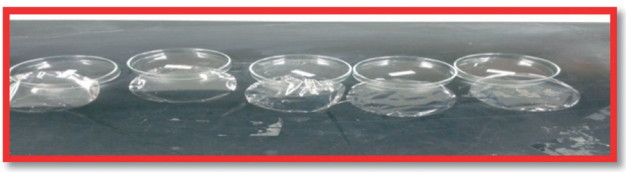

Fig. 15 Thin films after separation from Petri dish.

nanocomposite hydrogels having a porous surface morphology, which enables introduction of a relatively large load of drugs into them. The newly synthesized gel thin films were used for insulin drug delivery. It was observed that they apparently decreased the blood glucose concentration (50–65% of the initial blood glucose concentration) for at least 4–5.5 h after administration and they showed no cytotoxicity after administration.

Acknowledgements

The authors would like to express their sincere thanks to Umm Al-Qura University, Faculty of Science, Chemistry Department in the Kingdom of Saudi Arabia, where all experiments were performed in compliance with the relevant laws and guidelines, and the institutional committee(s) in Umm Al-Qura University has approved the experiments. Also, we direct our appreciation to King Khaled University, Faculty of Science, Saudi Arabia for performing the spectral analyses and to Pharmacognosy Department, Faculty of Pharmacy, Mansoura University for determining the biological activity of the tested hydrogels.

Notes and references

1 T. R. Hoare and D. S. Kohane, *Polymer*, 1993, **49**, 200.
2 N. A. Das, *Int. J. Pharm. Pharm. Sci.*, 2013, **5**(3), 112.
3 N. Chirani, L.-H. Yahia, L. Gritsch, F. L. Motta, S. Chirani and S. Fare, *J. Biomed. Sci.*, 2015, **4**(2:13), 1.
4 J. A. Burdick and G. D. Prestwich, *Adv. Mater.*, 2011, **23**, H41.
5 K. T. Nguyen and J. L. West, *Biomaterials*, 2002, **23**, 4307.
6 N. Sahiner, W. T. Godbey, G. L. McPherson and V. T. John, *Colloid Polym. Sci.*, 2006, **284**, 1121.
7 K. Y. Lee and D. J. Mooney, *Chem. Rev.*, 2001, **101**(7), 1869.
8 H. J. van der Linden, S. Herber, W. Olthuis and P. Bergveld, *Analyst*, 2003, **128**, 325.
9 A. C. Jen, M. C. Wake and A. G. Mikos, *Biotechnol. Bioeng.*, 1996, **50**(4), 357–362.
10 K. Wang, J. Burban and E. Cussler, Hydrogels as separation agents, *Responsive gels: volume transitions II*, 1993, vol. 67.
11 S. L. Bennett, D. A. Melanson, D. F. Torchiana, D. M. Wiseman and A. S. Sawhney, *J. Card. Surg.*, 2003, **18**(6), 494.
12 R. Lapasin and S. Pricl, *Rheology of industrial polysaccharides: theory and application*, Aspen Publication, New York, USA, 1999.
13 M. N. V. R. Kumar, *React. Funct. Polym.*, 2000, **46**, 1.
14 F. A. Al Sagheer, M. A. Al-Sughayer, S. Muslim and M. Z. Elsabee, *Carbohydr. Polym.*, 2009, **77**(1), 410.
15 D. Knorr, *Process Biochem.*, 1986, **6**, 90.
16 R. A. A. Muzzarelli, Filmogenic Properties of Chitin/Chitosan in *Chitin in Nature and Technology*, ed. R. A. A. Muzzarelli, C. Jeuniaux and G. W. Gooday, Plenum Press, New York, USA, 1986, pp. 389–396.
17 A. El Ghaouth, J. Arul, R. Ponnampalam and M. Boulet, *J. Food Sci.*, 1991, **56**, 1618.
18 R. M. Ottenbrite, K. Park, T. Okano and N. A. Peppas, *Biomedical Applications of Hydrogels Handbook*, Springer, New York, 2010.
19 N. B. Graham, Polyethylene glycol chemistry, in *Biotechnical and biomedical application*, ed. J. M. Harris, Plenum Press, New York, 1992, p. 1.
20 A. H. Krauland, D. Guggi and A. B. Schnurch, *Int. J. Pharm.*, 2006, **307**, 270.

